

# Ant Colony Sampling with GFlowNets for Combinatorial Optimization

Minsu Kim<sup>\*12</sup> Sanghyeok Choi<sup>\*2</sup> Jiwoo Son<sup>2</sup> Hyeonah Kim<sup>2</sup> Jinkyoo Park<sup>23</sup> Yoshua Bengio<sup>456</sup>

## Abstract

This paper introduces the Generative Flow Ant Colony Sampler (GFACS), a novel neural-guided meta-heuristic algorithm for combinatorial optimization. GFACS integrates generative flow networks (GFlowNets) with the ant colony optimization (ACO) methodology. GFlowNets, a generative model that learns a constructive policy in combinatorial spaces, enhance ACO by providing an informed prior distribution of decision variables conditioned on input graph instances. Furthermore, we introduce a novel combination of training tricks, including search-guided local exploration, energy normalization, and energy shaping to improve GFACS. Our experimental results demonstrate that GFACS outperforms baseline ACO algorithms in seven CO tasks and is competitive with problem-specific heuristics for vehicle routing problems. The source code is available at <https://github.com/ai4co/gfacs>.

## 1. Introduction

Combinatorial Optimization Problems (COPs) constitute a category of optimization problems focused on finding the optimal arrangement of discrete structures, such as sets, sequences, and graphs, that maximizes a given objective function. COPs are prevalent in various fields, including compiler scheduling (Zhang et al., 2022b) and hardware design (Kim et al., 2023b), but they are usually NP-hard. Over the decades, heuristics that quickly find near-optimal solutions have been developed to tackle this NP-hardness. However, these problem-specific heuristics require considerable effort and domain knowledge to make them effective. Thus, meta-heuristic algorithms, such as Ant Colony Optimization (ACO) (Dorigo et al., 2006), have been proposed to provide a more generalized approach to designing heuristics.

<sup>\*</sup>Equal contribution <sup>1</sup>Work performed while the author was at the Mila – Québec AI Institute <sup>2</sup>Korea Advanced Institute of Science and Technology <sup>3</sup>Omelet <sup>4</sup>Mila – Québec AI Institute <sup>5</sup>Université de Montréal <sup>6</sup>CIFAR. Correspondence to: Minsu Kim <min-su@kaist.ac.kr>.

*Under review.*

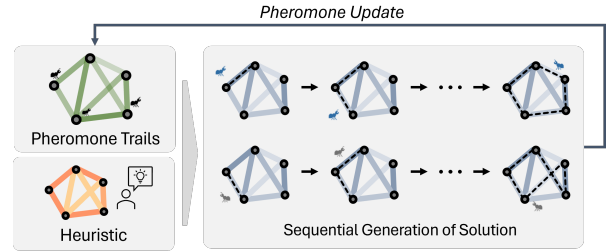


Figure 1. Illustration of ACO. Edge probability is obtained from the multiplication of heuristics and pheromone trails. Ants constructively complete solutions based on the edge probability, then update the pheromone trail with the constructed samples.

ACO is a meta-heuristic algorithm inspired by the foraging behaviors of ants, and it has demonstrated effectiveness in solving COPs and general optimization problems. In ACO, a population of artificial ants iteratively builds solutions and updates ‘pheromone trails’ to explore the solution space. At each iteration, solutions are constructed through stochastic moves guided by instance-specific pheromone trails and problem-specific heuristic measures indicating the goodness of sampling certain trails; see Figure 1 for an illustration. While the pheromone trails are updated based on solutions constructed during the iterative procedure of solving an instance, the heuristic measures typically need to be predefined in a matrix form (e.g., heat map). However, developing an effective heuristic matrix for ACO involves expert knowledge and manual tuning, posing challenges in less-explored problem domains where the expertise is limited.

Recently, a neural-guided Ant Colony Optimization (ACO) method, DeepACO, was introduced by Ye et al. (2023). This technique utilizes graph neural networks (GNN) (Joshi et al., 2021) to model the heuristic matrix of input instance graphs of COPs. Specifically, this framework is developed as a GNN-based policy that selects an edge (action) based on previously chosen edges (state). Then, the composited policy generates a state trajectory from an empty set (initial state) to a complete solution (terminal state), as in Figure 1. DeepACO incorporates reinforcement learning (RL) to train the GNN-based policy model with a reward signal from the terminal state of the generated trajectory. After RL training, the learned GNN is utilized to construct the heuristic matrix for a given problem instance, thereby providing a good prior

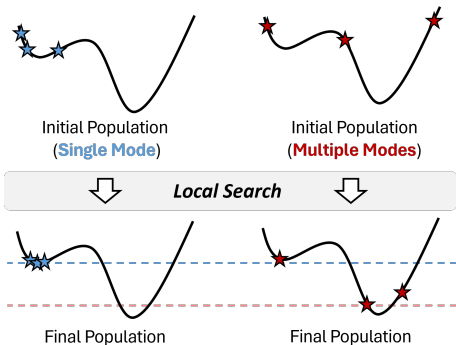


Figure 2. Importance of capturing multi-modality in combinatorial optimization with local search post-processing (●). The probability of improved solutions rises after local search, even from initially higher-cost samples, particularly with a sampler adept at capturing multi-modality.

to ACO to explore the solution space more efficiently. Note that the trained GNN acts as a parameterized prior, effectively transferring the solution exploration strategy obtained during training to each new instance.

However, we observe certain limitations in DeepACO, primarily in three aspects. The first limitation (●) is that the usage of a behavior policy is limited since DeepACO uses on-policy RL to train the graph representation. It potentially weakens the performance of heuristic matrices by limiting the choice of behavior policy, which is crucial for the effective exploration of massive combinatorial spaces. Secondly (●), the reward-maximizing RL of DeepACO fails to satisfactorily capture the diversity of solutions, i.e., the multi-modality of the solution landscape. In CO, a diversity of good candidates is highly advantageous, as it increases the chances of finding a global optimum after a local search; see Figure 2. Lastly (●), the inherent symmetry in combinatorial solutions, where multiple trajectories can lead to identical combinatorial outcomes, is challenging to consider in the context of RL. For example, in the Traveling Salesman Problem (TSP), distinct paths like (1,2,3,4) and (4,3,2,1) represent the same cyclic solution. As DRL methods train policy on a tree-structured MDP, each trajectory is identified as a different solution.

**Contribution.** This paper introduces a novel ACO algorithm, the Generative Flow Ant Colony Sampler (GFACS), which addresses the limitations of DeepACO by integrating the emerging amortized inference method of GFlowNets (Bengio et al., 2021; 2023). First (●), the off-policy training property of GFlowNets allows for the utilization of samples drawn from any behavior policy, including powerful heuristic search algorithms commonly used in COPs. Secondly (●), unlike maximum reward-seeking algorithms (e.g., RL training in DeepACO), GFlowNets are sampling algorithms and well-suited for modeling the multi-modality nature of

certain distributions. Lastly (●), GFlowNets, which model the solution generative process on a directed acyclic graph (DAG), incorporate the symmetry of combinatorial solutions by design (Bengio et al., 2023).

To adequately integrate GFlowNet into ACO, we propose an effective combination of training techniques. In our approach, we employ a strategic guided exploration with two distinct behavior policies to collect exploratory and exploitation samples. One aims for a diverse range of samples, and the other aims for locally optimized samples. This approach effectively addresses the over-exploration issue in GFlowNets, which often results in poor performances due to an excessive focus on diversity. To encourage further exploration, we introduce an energy reshaping to compensate samples that have initially high energy but can be significantly improved, as exemplified by the red samples in Figure 2. At last, a shared energy normalization is employed to stabilize the training of conditional GFlowNets, wherein the energy landscape is contingent upon the variability of input problems.

Our GFACS exhibits significant superiority over the current DeepACO and classical ACO algorithms for various representative CO tasks, which vehicle routing problems, scheduling problems, and a grouping problem. Moreover, GFACS outperforms or shows similar performance to competitive deep reinforcement learning-based vehicle routing solvers, which are designed to solve traveling salesman problems (TSP) and capacitated vehicle routing problems (CVRP) in the context of large-scale instances, such as  $N = 500, 1000$ .

## 2. Related Works

### 2.1. Ant Colony Optimization

Ant Colony Optimization (ACO) is a meta-heuristic inspired by ant behavior in finding optimal paths. Traditional ACO algorithms, such as Ant System (AS) (Dorigo et al., 1996) and MAX-MIN AS (Stützle & Hoos, 2000), rely on specific heuristics for success. To reduce the reliance on heuristic design, Ye et al. (2023) introduce a neural-guided ACO, called DeepACO, utilizing graph representation learning and reinforcement learning to replace manual heuristics with automatically acquired knowledge.

### 2.2. Neural Combinatorial Optimization

Neural combinatorial optimization (Bello et al., 2016) is a deep learning-based method to train an instance-conditional policy using supervised learning (Vinyals et al., 2015; Fu et al., 2021; Sun & Yang, 2023) or unsupervised learning (Khalil et al., 2017; Kool et al., 2018; Kwon et al., 2020). Usually, supervised learning methods are beneficial when the target problem has an accurate but time-consuming ex-

pert solver. The oracle-labeled data is collected from the oracle solvers, and deep neural networks amortize them, allowing for scalability and faster inferences than the expert solver. On the other hand, unsupervised learning proceeds through self-guided trial and error, using the COP objective as a training signal. This makes it applicable even if encountering less-studied problems where powerful expert solvers are unavailable (Bello et al., 2016; Ahn et al., 2020). Our method can be categorized as an unsupervised learning method, which does not need expert labels. See Appendix F for a more comprehensive survey.

### 2.3. GFlowNets and Combinatorial Optimization

GFlowNets, tailored for sampling combinatorial objects proportionally to a given reward function, play a pivotal role in diversifying the candidate pool for molecule generation in crucial areas like drug discovery (Bengio et al., 2021). Recent efforts to advance GFlowNets have focused on developing new training objectives (Malkin et al., 2022; Madan et al., 2022; Zhang et al., 2023b), enhancing credit assignment (Pan et al., 2023a; Jang et al., 2024), and improving exploration strategies (Pan et al., 2022; Rector-Brooks et al., 2023; Pan et al., 2023a; Kim et al., 2023d;c). Our contribution lies in proposing an efficient exploration technique tailored for combinatorial optimization problems.

GFlowNets have also found successful applications in some COPs (Zhang et al., 2022b; 2023a). Zhang et al. (2023a) effectively addresses the symmetric nature of graph constraint optimization, showcasing remarkable performance in graph CO tasks like maximum independent sets. Zhang et al. (2022b) solves proxy-based scheduling problems. Despite their success, their method has limited applications to either locally decomposable graph CO problems (Ahn et al., 2020) or robust scheduling problems. Our method is a neural-guided meta-heuristic, which aims to be a general-purpose CO solver. Additionally, this paper appears to be the first to address the traveling salesman problem and its variations using GFlowNets. These tasks present a significant challenge due to the global constraints to compare with graph CO tasks.

## 3. Preliminary

### 3.1. Travelling Salesman Problem

The traveling salesman problem (TSP) is a fundamental combinatorial optimization problem, which serves as a building block for more complex CO problems like the capacitated vehicle routing problem (CVRP) and orienteering problem (OP). In light of this and for simplicity, this paper presents formulations using the two-dimensional Euclidean TSP as an illustrative example. Note that the formulations can be extended to other COPs straightforwardly.

A TSP instance is defined on a (fully connected) graph  $\mathcal{G} = \{\mathcal{V}, \mathcal{D}\}$ , where  $\mathcal{V}$  and  $\mathcal{D}$  are a node set and edge set, respectively. Each node  $i \in \mathcal{V}$  has two-dimensional coordinates  $v_i \in [0, 1]^2$  as a feature, and each edge  $(i, j) \in \mathcal{D}$  has a feature  $d_{i,j}$  which is the distance between node  $i$  and  $j$ , i.e.,  $d_{i,j} = \|v_i - v_j\|_2$ . A solution to TSP,  $x(\mathcal{G})$  corresponds to a Hamiltonian cycle for a given problem instance  $\mathcal{G}$ , which can be represented as a permutation of nodes  $\pi = (\pi_1, \dots, \pi_N)$ . The tour length is computed as  $f(x(\mathcal{G})) = \sum_{t=1}^{N-1} d_{\pi_t, \pi_{t+1}} + d_{\pi_N, \pi_1}$ . The optimization objective for TSP is to find  $x(\mathcal{G})$  that minimizes  $f(\cdot, \mathcal{G})$ .

### 3.2. Ant Colony Optimization

Ant colony optimization is a meta-heuristic to refine the solution sampling probability by an iterative procedure of solution construction and pheromone update. Given a problem instance  $\mathcal{G}$ , a corresponding heuristic matrix  $\eta(\mathcal{G}) \in \mathbb{R}^{N \times N}$  and a pheromone trails  $\rho \in \mathbb{R}^{N \times N}$ , a solution is constructed by auto-regressively sampling edges from the probability distribution:

$$P(\pi_{t+1} = j | \pi_t = i; \rho, \eta(\mathcal{G})) \propto \begin{cases} \rho_{i,j} \eta_{i,j}(\mathcal{G}) & \text{if } j \notin \pi_{1:t} \\ 0 & \text{otherwise,} \end{cases} \quad (1)$$

where  $\rho_{i,j}$  and  $\eta_{i,j}(\mathcal{G})$  are the pheromone weight and heuristic weight for edge  $d_{i,j}$ , respectively.

At each iteration,  $K$  artificial ants independently sample solutions  $\{\pi^k\}_{k=1}^K$  by following Equation (1). The pheromone trails  $\rho$  are then adjusted using the solution set and corresponding costs, thereby updating the solution construction probability. The pheromone update rules vary depending on the ACO algorithm used. For example, in Ant System (AS) (Dorigo et al., 1996), all  $K$  solutions contribute to the pheromone update:

$$\rho_{i,j} \leftarrow (1 - \gamma)\rho_{i,j} + \sum_{k=1}^K \Delta_{i,j}^k, \quad (2)$$

where  $\gamma$  is the decaying coefficient (or evaporation rate) and  $\Delta_{i,j}^k$  is the amount of pheromone laid by the  $k$ -th ant on the edge  $(i, j)$ . Here,  $\Delta_{i,j}^k$  is proportional to the inverse of tour length if  $(i, j)$  is included in  $\pi^k$ , and zero otherwise.

Note that the heuristic matrix  $\eta(\mathcal{G}) \in \mathbb{R}^{N \times N}$  is not updated during the search process, only serving as a prior. Thus, ACO aligns the search process more closely with the most efficacious paths discovered; see Dorigo et al. (2006) for details. In DeepACO (Ye et al., 2023), the learned GNN, parameterized by  $\theta$ , is utilized to construct the heuristic matrix  $\eta(\mathcal{G}, \theta)$  for a given problem instance  $\mathcal{G}$ , thereby providing a good prior for exploring the solution space.

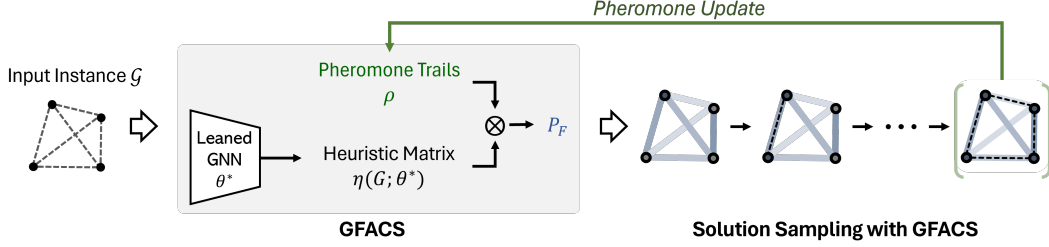


Figure 3. Solution sampling process of GFACS. The GNN is trained with GFlowNets and serves as an expert heuristic in GFACS.

### 3.3. Generative Flow Networks

Generative Flow Networks, or GFlowNets (Bengio et al., 2021; 2023) provide an effective training framework for learning a policy that samples compositional objects denoted as  $x \in \mathcal{X}$ . GFlowNets follow a constructive generative process, using discrete *actions* to iteratively modify a *state* which represents a partially constructed object. All the ways to construct these objects can be described by a directed acyclic graph (DAG),  $\mathcal{H} = (\mathcal{S}, \mathcal{A})$ , where  $\mathcal{S}$  is a finite set of all possible states, and  $\mathcal{A}$  is a subset of  $\mathcal{S} \times \mathcal{S}$ , representing directed edges. Within this framework, we define the *children* of state  $s \in \mathcal{S}$  as the set of states connected by edges whose head is  $s$ , and the *parents* of state  $s$  as the set of states connected by edges whose tail is  $s$ .

We define a *complete trajectory*  $\tau = (s_0 \rightarrow \dots \rightarrow s_N) \in \mathcal{T}$  from the initial state  $s_0$  to terminal state  $s_N$ . We denote  $\tau_{\rightarrow x}$  when the terminal state  $s_N$  is finalized to the corresponding object  $x \in \mathcal{X}$ . We define the *forward policy* to model the forward transition probability  $P_F(s'|s)$  from  $s$  to its child  $s'$ . Similarly, we also consider the *backward policy*  $P_B(s|s')$  for the backward transition  $s' \dashrightarrow s$ , where  $s$  is a parent of  $s'$ . We can use the *forward policy* to compute in a forward way the probability of a trajectory:

$$P_F(\tau; \theta) = \prod_{t=1}^n P_F(s_t | s_{t-1}; \theta) \quad (3)$$

Similarly, we can use the *backward policy* to compute in a backward way the probability of trajectory ending at a given object  $x$ :

$$P_B(\tau_{\rightarrow x} | x; \theta) = \prod_{t=1}^n P_B(s_{t-1} | s_t; \theta) \quad (4)$$

**Trajectory balance (Malkin et al., 2022).** Trajectory balance is the most widely used learning objective in a GFlowNet framework. When the trajectory balance objective is minimized, we achieve that the probability of sampling  $x$  with the forward policy is  $P_F^\top(x) \propto R(x)$ , as desired, where  $P_F^\top(x) = \sum_{\tau_{\rightarrow x} \in \mathcal{T}} P_F(\tau)$ . The trajectory balance loss  $\mathcal{L}_{\text{TB}}$  works by training three models, a learnable scalar  $Z_\theta$  for the partition function, a forward policy

$P_F(\tau; \theta)$ , and a backward policy  $P_B(\tau_{\rightarrow x} | x; \theta)$  to minimize the following objective:

$$\mathcal{L}_{\text{TB}}(\tau; \theta) = \left( \log \frac{Z_\theta P_F(\tau; \theta)}{R(x) P_B(\tau_{\rightarrow x} | x; \theta)} \right)^2 \quad (5)$$

## 4. Generative Flow Ant Colony Sampler

### 4.1. MDP formulation

This subsection formulates a Markov decision process (MDP) by using TSP as an example, similar to the preliminaries. A TSP solution is obtained through the sequential decision-making process of GFlowNets as follows:

**State  $s$ :** The initial state  $s_0$  is an empty set. The state  $s_t$  at  $t > 0$  is a sequence of previous actions:  $(a_0, \dots, a_{t-1})$ .

**Action  $a$ :** The action  $a_t$  is a selection of a node to visit at time  $t$  among un-visited nodes:  $a_t \in \{1, \dots, N\} \setminus \{a_0, \dots, a_{t-1}\}$ . If all nodes are visited, a deterministic terminating action is applied, which maps a final state  $s_N$  into a solution,  $x(\mathcal{G})$ .

**Reward  $R(x(\mathcal{G}); \beta)$ :** The reward is defined as the unnormalized energy distribution of the solution  $x(\mathcal{G})$ , i.e.,

$$R(x(\mathcal{G}); \beta) = e^{-\beta \mathcal{E}(x(\mathcal{G}))} = e^{-\beta f(x(\mathcal{G}))}. \quad (6)$$

Here,  $\mathcal{E}(x(\mathcal{G}))$  is energy for solution  $x(\mathcal{G})$ , which is the same as the tour length of the solution for TSP, i.e.,  $\mathcal{E}(x(\mathcal{G})) = f(x(\mathcal{G}))$ . The  $\beta$  is the inverse energy temperature, which is a hyperparameter.

### 4.2. Policy Configuration

We parameterize the forward policy  $P_F$  using a graph neural network (GNN) with parameter  $\theta$  that maps an input graph instance  $\mathcal{G}$  to the output edge feature  $\eta(\mathcal{G}; \theta)$ , following Ye et al. (2023). Then, the forward policy when  $t < N$  is expressed as follows:

$$P_F(s_{t+1} | s_t; \eta(\mathcal{G}; \theta), \rho) \propto \begin{cases} \rho_{a_{t-1}, a_t} \eta_{a_{t-1}, a_t}(\mathcal{G}; \theta) & \text{if } a_t \notin s_t \\ 0 & \text{otherwise} \end{cases} \quad (7)$$

Note that  $\rho$  and  $\eta(\mathcal{G}; \theta)$  denote the pheromone trails and learned heuristic matrix in ACO.

Subsequently, we can define a trajectory from the initial state to a terminal solution  $\tau = (s_0, \dots, s_N, x(\mathcal{G}))$  and the forward probability of that trajectory:

$$P_F(\tau; \eta(\mathcal{G}; \theta), \rho) = \prod_{t=0}^{N-1} P_F(s_{t+1}|s_t; \eta(\mathcal{G}; \theta), \rho) \quad (8)$$

Note that the forward probability for the transition from  $s_N$  to  $x(\mathcal{G})$  is omitted as it follows a deterministic rule.

For the backward policy, we set  $P_B = \frac{1}{2N}$ , emulating the maximum entropy GFlowNets (Zhang et al., 2022a) to make uniform exploration over symmetric trajectories which terminate into identical solution. Here,  $P_B$  represents a uniform distribution across all  $2N$  feasible trajectories leading to a solution  $x(\mathcal{G})$ . This is particularly pertinent in the context of the TSP involving  $N$  cities, where  $2N$  permutations culminate in the same Hamiltonian cycle  $x(\mathcal{G})$ . The count of symmetric trajectories depends on the task’s characteristics. For an exhaustive discussion on solution symmetry across various COPs, please refer to Appendix E.

### 4.3. Solution Sampling with GFACS

In the sampling process, we assume the existence of the learned GNN parameterized with  $\theta^*$ ; see Section 5 for details of the training procedure. The learned GNN provides the heuristic matrix  $\eta(\mathcal{G}; \theta^*)$  for ACO algorithm. Thus, the remaining process is to update pheromone parameter  $\rho$  with solutions sampled by  $P_F(\tau; \eta(\mathcal{G}; \theta^*), \rho)$  during the solution searching process. As the  $\eta(\mathcal{G}; \theta^*)$  is trained with GFlowNets to sample diverse high-rewarded (i.e., low energy) samples,  $P_F$  generates good candidates for updating  $\rho$ . The overall process is illustrated in Figure 3.

## 5. Training GFACS

This section introduces how to train GFACS, especially the GNN component  $\theta$ , in the GFlowNet framework. GFACS is trained via iterations of the following two steps. First (**Step A**; Section 5.1), we collect experiences, each being a triplet of input instance graph  $\mathcal{G}$ , a complete trajectory  $\tau_{\rightarrow x(\mathcal{G})}$ , and the energy of the solution  $\mathcal{E}(x(\mathcal{G}))$ . We employ  $\beta$  annealing and guided exploration for better exploration and energy reshaping for proper credit assignment. Next (**Step B**; Section 5.1), the parameterized forward policy  $P_F$  is trained using the collected experiences. Here, we utilize a shared energy normalization to stabilize training.

### 5.1. Step A: Experience Collection

For every iteration, we first sample  $M$  problem instances from a random sampler  $P(\mathcal{G})$ , i.e.,  $\mathcal{G}_1, \dots, \mathcal{G}_M \sim P(\mathcal{G})$ .

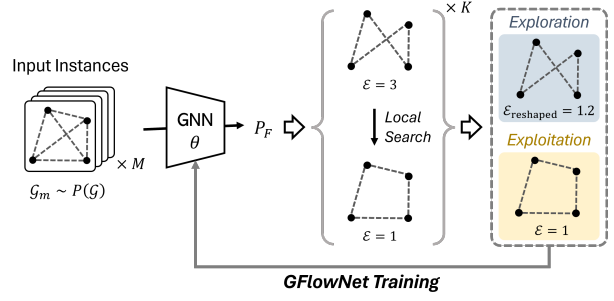


Figure 4. Training of GFACS using GFlowNets and our novel training tricks of guided exploration and energy reshaping.

Details of instance sampling are described in Appendix B.

**Collecting exploration samples with  $\beta$  annealing.** For each problem instance  $\mathcal{G}_m$ , we collect  $K$  exploration solutions by following Eq. 8, resulting in an exploration batch,  $\mathcal{B}_{\text{explore}} = \{(\mathcal{G}_m, \tau_{\rightarrow x_{m,k}}, \mathcal{E}(x_{m,k}))\}_{m=1, \dots, M, k=1, \dots, K}$ . To encourage exploration for solution sampling, we introduce an annealing scheme for the inverse energy temperature  $\beta$ . Rather than set the  $\beta$  to a fixed value, we gradually increase the beta toward the target value along the training procedure. This makes the policy in the early stage of training to be exploratory, preventing it from getting stuck into a local optimum.

**Collecting exploitation samples with guided exploration.** To cope with the over-exploration problem of GFlowNet, we also collect  $K$  exploitation samples for each  $\mathcal{G}_m$  using guided exploration. We use a heuristic local search operator ( $LS$ ), such as 2-opt for TSP, as external guidance. The local search operator directly refines a given solution into a locally optimized one, i.e.,  $x' \leftarrow LS(x)$ . We then use  $P_B$  to collect a trajectory  $\tau_{\rightarrow x'}$  for each  $x'$ , obtaining a batch of exploitation experiences,  $\mathcal{B}_{\text{exploit}} = \{(\mathcal{G}_m, \tau_{\rightarrow x'_{m,k}}, \mathcal{E}(x'_{m,k}))\}_{m=1, \dots, M, k=1, \dots, K}$ .

However, a powerful local search operator may not exist for some problems, especially for less-explored ones. In such cases, we use the Top- $L$  guidance technique, described as follows. For a given problem instance  $\mathcal{G}_m$ , we first update the pheromone trails using the exploration samples collected before. After that,  $L \times K$  new sample solutions are generated with the updated pheromone, where  $L$  is a hyperparameter. Among the new samples, we select top  $L$  solutions with the lowest energy and also select  $(K - L)$  random solutions, resulting in  $K$  exploitation samples for each  $\mathcal{G}_m$ , and thus obtaining  $\mathcal{B}_{\text{exploit}}$  like before.

**Energy reshaping for exploratory samples.** In the case where we have a local search operator, we reshape the energy for the exploration  $x$  in  $\mathcal{B}_{\text{explore}}$  using the energy of the refined solution  $x' = LS(x)$  as follows:

$$\mathcal{E}_{\text{reshaped}}(x) = \alpha \mathcal{E}(x') + (1 - \alpha) \mathcal{E}(x) \quad (9)$$

This is to evaluate an underrated sample that initially had high energy (i.e., low reward) but can be easily changed to have low energy (i.e., high reward) after the local search (see Figure 2). This reshaping changes the reward values in  $\mathcal{B}_{\text{explore}}$  accordingly, while  $\mathcal{B}_{\text{exploit}}$  remains the same. Note that this reshaping cannot be applied for  $\text{TopK}$  guidance because  $x'$  cannot be determined solely with  $x$  in that case.

## 5.2. Step B: Training with Collected Experiences

Given the collected experience batches  $\mathcal{B}_{\text{explore}}$  and  $\mathcal{B}_{\text{exploit}}$ , we aim to minimize the following loss function:

$$\mathcal{L}(\theta) = \mathcal{L}(\theta; \mathcal{B}_{\text{explore}}) + \mathcal{L}(\theta; \mathcal{B}_{\text{exploit}}), \quad (10)$$

where  $\mathcal{L}(\theta; \mathcal{B})$

$$= \sum_{m=1}^M \sum_{k=1}^K \left( \log \frac{2N P_F(\tau_{\rightarrow x_{m,k}}^m; \eta(\mathcal{G}_m; \theta), \rho) Z_\theta(\mathcal{G}_m)}{R(x_{m,k}; \beta)} \right)^2. \quad (11)$$

The  $2N$  comes from the fact that TSP has  $2N$  permutations, as discussed in Section 4.2. In addition, our target sampling distribution is proportional to reward  $p(x; \mathcal{G}) \propto R(x(\mathcal{G}))$ . However, in most COPs, including TSP, the scale of  $R(x(\mathcal{G}))$  is significantly different, possibly leading to unstable training due to the high variance of rewards. Similarly to previous works that stabilize REINFORCE training (Kwon et al., 2020; Kim et al., 2022b), we normalize the energy  $\mathcal{E} = -\log R$  using the sample mean over a  $K$  samples for the same  $\mathcal{G}_m$ , i.e.,

$$-\log \tilde{R}(x_{m,k}) = \tilde{\mathcal{E}}(x_{m,k}) = \mathcal{E}(x_{m,k}) - \frac{1}{K} \sum_{k=1}^K \mathcal{E}(x_{m,k}). \quad (12)$$

We call this technique a shared energy normalization. Note that the shared energy normalization is applied independently to the two batches,  $\mathcal{B}_{\text{explore}}$  and  $\mathcal{B}_{\text{exploit}}$ , as the energy distribution between the two batches is often significantly different to each other, especially when a heuristic local search is applied.

## 6. Experiments

This section presents the experimental findings of the GFACS framework. First, we test GFACS against established ACO baselines in various CO tasks. Subsequently, we explore the trade-offs between diversity and optimality in relation to the inverse energy temperature  $\beta$ . Next, an ablation study is conducted to evaluate the effectiveness of our proposed training techniques. Lastly, we compare GFACS with the RL-based combinatorial optimization methods in two representative routing problems, the TSP and the capacitated vehicle routing problem (CVRP).

### 6.1. Setup

**Implementation and hyperparameters.** GFACS is built upon the implementation established by DeepACO (Ye et al., 2023). As our methodology mainly focuses on improving training algorithms rather than network architecture, we simply adopt the GNN architecture proposed in DeepACO, except the additional parameters for partition function  $Z_\theta$  in Eq. 11. For detailed network architecture and hyperparameters, please refer to Appendix A. One important hyperparameter that GFACS newly introduces is the inverse energy temperature  $\beta$ , described in Eq. 6. We offer an analysis of the impact and significance of  $\beta$  in Section 6.4.

**Test settings.** Each algorithm is tested on the held-out datasets generated or obtained in advance. Unless otherwise stated, the results presented throughout this section are the averaged values from three independent models, each trained with a distinct random seed.

### 6.2. Comparison with ACO algorithms

Here, we compare GFACS against the classical ACO and the recent DeepACO algorithm across various CO tasks.

**Problems.** Following the approach of Ye et al. (2023), we evaluate our algorithm in a range of COPs. This includes four routing problems – TSP, Capacitated Vehicle Routing Problem (CVRP), Prize-Collecting Vehicle Routing Problem (PCTSP), and Orienteering Problem (OP) – along with two scheduling problems – Sequence Ordering Problem (SOP) and Single Machine Total Weighted Tardiness Problem (SMTWTP) – and a grouping problem, the Bin Packing Problem (BPP). For detailed problem configurations, we direct readers to Appendix B or Ye et al. (2023) as we mostly follow their problem settings. For TSP and CVRP, we use local search algorithms with neural-guided perturbation following Ye et al. (2023). For other problems, we use  $\text{TopK}$  guidance as described in Section 5.1.

**Baselines.** We use ACO and DeepACO as baseline algorithms. Both baselines and GFACS use Ant System (Dorigo et al., 1996) for pheromone update (Eq. 2). We also test GFACS without guided exploration to analyze its effect on the performance. We use 100 ants and  $T = 100$  ACO iterations for all the algorithms.

**Results.** As shown in Figure 5, GFACS consistently surpasses both the classic ACO algorithm and DeepACO across all benchmark problems. Especially for routing problems, GFACS outperforms DeepACO by a considerable margin. This is particularly remarkable given that both algorithms utilize identical neural networks and local search operators, highlighting the crucial role of our training strategy. Without guided exploration, GFACS generally performs badly, likely due to the over-exploration problem of GFlowNets. This issue is effectively mitigated with the proposed guided

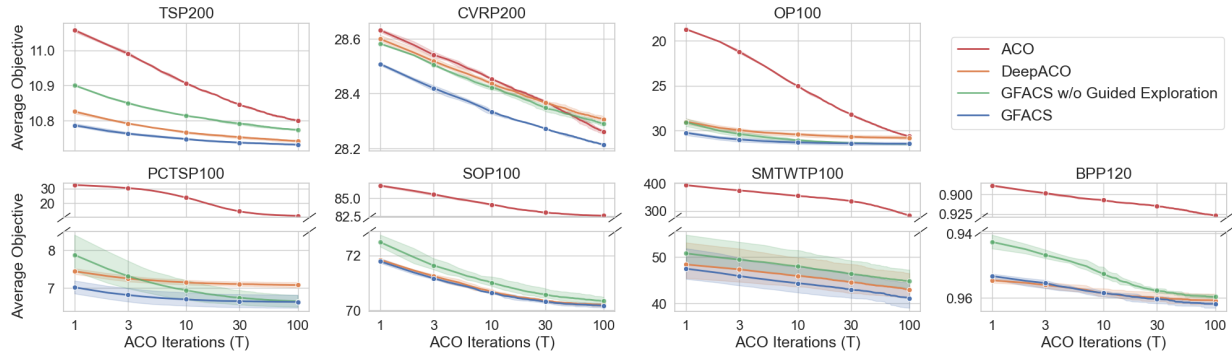


Figure 5. Results of ACO algorithms on various CO tasks. Our GFACS outperforms every ACO baseline. The results are averaged over 3 independent models evaluated on the held-out test sets, and the shade indicates the min-max range of the 3 models. GFACS, without guided exploration, gives poorer performances. This verifies the effectiveness of our algorithm.

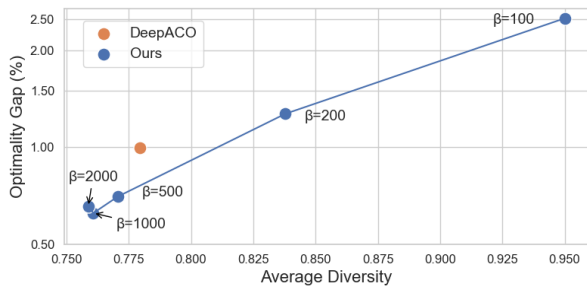


Figure 6. The trade-off between diversity and optimality as the inverse energy temperature  $\beta$  changes. By adjusting  $\beta$ , we can control the trade-off of having a Pareto frontier to compare with DeepACO. The reported values are obtained with  $T = 1$ , i.e., the solutions are not affected by the pheromone.

exploration, showing the efficacy of our method. Interestingly, in CVRP, OP, and PCTSP, GFACS without guided exploration outperforms DeepACO after a certain number of ACO iterations. We believe that this is attributed to the increased solution diversity of GFACS, which comes from the generative nature of the policy and implied DAG structure that incorporates the solution symmetry.

### 6.3. Analysis of $\beta$ and Diversity-Optimality Trade-off

In this subsection, we explored the diversity-optimality trade-off by varying the inverse energy temperature  $\beta$  (Eq. 6) from low to high values. For analysis, we generate  $K$  solution samples from policies trained with GFACS with different values of  $\beta$  and DeepACO (with  $\rho = 1$  so that the pheromone does not affect the result). We use average pairwise Jaccard distance as a diversity metric (formally defined in Appendix D). Results for TSP200 (Figure 6) show that lower  $\beta$  values lead to more diverse but less optimal solutions, while higher  $\beta$  values result in less diversity but higher optimality. GFACS confirms the anticipated trade-off between diversity and optimality, establishing a Pareto frontier over DeepACO by offering more diverse and high-quality

Table 1. An ablation study examining various design elements of our method for TSP200 and CVRP200. Here, the optimality gap is used as a metric, where lower values indicate better performance.

Method	TSP200	CVRP200
Ours	<b>0.26%</b>	<b>1.09%</b>
– $\beta$ annealing	0.27%	1.11%
– guided exploration	0.88%	1.42%
– energy reshaping	0.59%	<b>1.09%</b>
– shared energy normalization	3.11%	2.88%

solutions. This advantage is particularly beneficial when an effective local search mechanism is available, increasing the likelihood of achieving superior local optima, as illustrated in Figure 2. However, excessively high  $\beta$  (e.g., 2000 in our result) degrades the optimality, supposedly because too high  $\beta$  value prevents exploration during training, which in turn results in sub-optimality. This empirical evidence supports our design choice of  $\beta$  annealing, which encourages exploration in the early stage of training.

### 6.4. Ablation Study

We also conducted an ablation study for four key training techniques introduced in Section 5:  $\beta$  annealing, guided exploration, energy reshaping, and shared energy normalization. The ablation for  $\beta$  annealing is conducted by fixing  $\beta$  to the maximum value of the annealed  $\beta$  schedule, while for other elements, we simply remove them from our algorithm. The empirical results for TSP200 and CVRP200 reported in Table 1 validate the effectiveness of our design choices.

### 6.5. Comparison with Other Reinforcement Learning Methods for Combinatorial Optimization

In the domain of machine learning for combinatorial optimization, significant strides have been made using various approaches, including sampling-based methods (Sun et al., 2023), heatmap-guided searches (Sun & Yang, 2023; Qiu et al., 2022), and constructive methods that employ

Table 2. Experimental result on TSP. Results for methods with \* are drawn from Ye et al. (2023), Cheng et al. (2023a), and Jin et al. (2023). The reported time is the average computation time for solving a single instance.

Method	TSP200			TSP500			TSP1000		
	Obj.	Gap(%)	Time(s)	Obj.	Gap(%)	Times(s)	Obj.	Gap(%)	Time(s)
LKH-3	10.72	0.00	9.80	16.55	0.00	31.70	23.14	0.00	102
AM*	12.00	11.91	0.2	21.46	29.07	0.6	33.55	45.10	1.5
POMO*	10.89	1.62	0.10	20.57	24.40	0.6	32.90	42.30	4.1
POMO + EAS	10.75	0.30	120	18.25	10.27	300	30.77	32.96	600
POMO + SGBS	10.77	0.43	133	18.86	13.96	318	28.58	23.51	605
DIMES+MCTS*	-	-	-	17.01	2.78	11	24.45	5.75	32
SO*	10.78	0.63	10	16.94	2.40	15	23.77	2.80	26
Pointerformer*	10.79	0.68	5.5	17.14	3.56	14	24.80	7.90	40
H-TSP*	-	-	-	-	-	-	24.65	6.62	0.3
ACO ( $T = 10$ )	10.91	1.76	2.1	17.38	5.02	14	24.76	6.99	57
DeepACO ( $T = 10$ )	10.77	0.45	2.5	16.84	1.75	15	23.78	2.77	66
GFACS ( $T = 10$ )	<b>10.75</b>	<b>0.26</b>	2.5	<b>16.80</b>	<b>1.54</b>	15	<b>23.72</b>	<b>2.53</b>	66

Table 3. Experimental result on CVRP. The reported time is the average computation time for solving a single instance.

Method	CVRP200			CVRP500			CVRP1000		
	Obj.	Gap(%)	Time	Obj.	Gap(%)	Time	Obj.	Gap(%)	Time
LKH-3	28.02	0.00	2.4m	63.07	0.00	18.6m	119.52	0.00	2.1h
POMO	29.12	3.94	1s	68.69	8.90	2s	145.74	21.94	3s
POMO + EAS	<b>27.99</b>	<b>-0.11</b>	2.0m	64.76	2.67	5.0m	126.25	5.63	10.0m
POMO + SGBS	28.07	0.19	2.0m	65.44	3.75	5.2m	127.90	7.01	10.1m
SymNCO	29.15	4.03	1s	68.81	9.10	2s	141.82	18.66	3s
SymNCO + EAS	28.01	0.27	2.0m	64.63	2.47	5.0m	125.58	5.07	10.0m
SymNCO + SGBS	28.10	0.30	2.0m	65.40	3.69	5.2m	127.53	6.70	10.1m
ACO ( $T = 10$ )	28.45	1.55	13s	64.62	2.45	36s	122.82	2.76	1.3m
DeepACO ( $T = 10$ )	28.44	1.49	14s	64.49	2.25	36s	122.15	2.20	1.3m
GFACS ( $T = 10$ )	28.32	1.09	14s	<b>64.19</b>	<b>1.76</b>	36s	<b>121.80</b>	<b>1.91</b>	1.3m

(Drakulic et al., 2023; Kool et al., 2018; Kwon et al., 2020). Our study compares our methods with RL-based approaches in TSP and CVRP for sizes  $N = 200, 500, 1000$ , which do not require expert-labeled data. This comparison is particularly relevant as our unsupervised approach aligns with sequence decision-making processes akin to RL.

**Baselines.** For TSP baselines, we select the AM (Kool et al., 2018), POMO (Kwon et al., 2020), Sym-NCO (Kim et al., 2022b) and Pointerformer (Jin et al., 2023) as RL-based constructive methods, DIMES (Qiu et al., 2022) as RL-based heatmap-based methods, the Select and Optimize (SO) (Cheng et al., 2023b) as RL-based improvement methods, and H-TSP (Pan et al., 2023b) as a RL-based hierarchical methods. We also applied two search algorithms, the Efficient Active Search (EAS) (Hottung et al., 2021) and Simulation Guided Beam Search (SGBS) (Choo et al., 2022), to POMO for a more thorough comparison. For CVRP<sup>1</sup>. We choose POMO and Sym-NCO as baselines with EAS and SGBS. Note that we restrict the duration of these searches to no more than 2, 5, and 10 minutes for prob-

lems with 200, 500, and 1000 nodes, respectively. We use LKH-3 (Helsgaun, 2017) as an oracle heuristic solver for TSP and CVRP to obtain near-optimal solutions that serve as baselines with 0.00% gap. Please refer to Appendix A.4 for the parameter settings of LKH-3.

**Results.** Among the baseline methods evaluated, our GFACS algorithm consistently delivers either superior or highly competitive performances. When compared to faster methods like AM, POMO or H-TSP, GFACS demonstrates substantially better results. Even after an additional search with EAS or SGBS, they fail to match GFACS’s achievements, except in CVRP200. Compared to algorithms like DIMES and Pointerformer, which operate at similar speeds, GFACS achieves improved performance. GFACS performs slightly worse than the oracle heuristic solver LKH-3, but offers an advantage of faster inference, especially in CVRP. Therefore, we can conclude that GFACS, as a general-purpose algorithm, holds significant appeal in the highly competitive benchmarks of both TSP and CVRP.

<sup>1</sup>We also adopt TAM as a CVRP baseline; however, due to the inaccessibility of source code, we compare it using the reported result in the paper (Hou et al., 2022). See Appendix C.2.



## 7. Conclusion

This paper proposes a novel neural-guided meta-heuristic algorithm called generative flow ant colony sampler (GFACS). Our algorithm was designed by integrating generative flow networks (GFlowNets) and ant colony optimization (ACO) with a novel combination of training techniques. GFACS consistently outperforms other ACO methods in several representative combinatorial optimization tasks. GFACS also shows competitive results both in traveling salesman problems and capacitated vehicle routing problems compared to a range of RL-based methods.

## References

- Ahn, S., Seo, Y., and Shin, J. Learning what to defer for maximum independent sets. In *International Conference on Machine Learning*, pp. 134–144. PMLR, 2020.
- Bello, I., Pham, H., Le, Q. V., Norouzi, M., and Bengio, S. Neural combinatorial optimization with reinforcement learning. *arXiv preprint arXiv:1611.09940*, 2016.
- Bengio, E., Jain, M., Korablyov, M., Precup, D., and Bengio, Y. Flow network based generative models for non-iterative diverse candidate generation. *Advances in Neural Information Processing Systems*, 34:27381–27394, 2021.
- Bengio, Y., Lahlou, S., Deleu, T., Hu, E. J., Tiwari, M., and Bengio, E. Gflownet foundations. *Journal of Machine Learning Research*, 24(210):1–55, 2023.
- Cheng, H., Zheng, H., Cong, Y., Jiang, W., and Pu, S. Select and optimize: Learning to solve large-scale tsp instances. In *International Conference on Artificial Intelligence and Statistics*, pp. 1219–1231. PMLR, 2023a.
- Cheng, H., Zheng, H., Cong, Y., Jiang, W., and Pu, S. Select and optimize: Learning to solve large-scale tsp instances. In Ruiz, F., Dy, J., and van de Meent, J.-W. (eds.), *Proceedings of The 26th International Conference on Artificial Intelligence and Statistics*, volume 206 of *Proceedings of Machine Learning Research*, pp. 1219–1231. PMLR, 25–27 Apr 2023b. URL <https://proceedings.mlr.press/v206/cheng23a.html>.
- Choo, J., Kwon, Y.-D., Kim, J., Jae, J., Hottung, A., Tierney, K., and Gwon, Y. Simulation-guided beam search for neural combinatorial optimization. *Advances in Neural Information Processing Systems*, 35:8760–8772, 2022.
- Croes, A. A method for solving traveling salesman problems. *Operations Research*, 5:791–812, 1958.
- d O Costa, P. R., Rhuggenaath, J., Zhang, Y., and Akcay, A. Learning 2-opt heuristics for the traveling salesman problem via deep reinforcement learning. In *Asian conference on machine learning*, pp. 465–480. PMLR, 2020.
- Dorigo, M., Maniezzo, V., and Colomi, A. Ant system: optimization by a colony of cooperating agents. *IEEE Transactions on Systems, Man, and Cybernetics, Part B (Cybernetics)*, 26(1):29–41, 1996. doi: 10.1109/3477.484436.
- Dorigo, M., Birattari, M., and Stutzle, T. Ant colony optimization. *IEEE Computational Intelligence Magazine*, 1(4):28–39, 2006. doi: 10.1109/MCI.2006.329691.
- Drakulic, D., Michel, S., Mai, F., Sors, A., and Andreoli, J.-M. Bq-ncq: Bisimulation quotienting for generalizable neural combinatorial optimization. *arXiv preprint arXiv:2301.03313*, 2023.
- Elfving, S., Uchibe, E., and Doya, K. Sigmoid-weighted linear units for neural network function approximation in reinforcement learning. *Neural networks*, 107:3–11, 2018.
- Fischetti, M., Gonzalez, J. J. S., and Toth, P. Solving the orienteering problem through branch-and-cut. *INFORMS Journal on Computing*, 10(2):133–148, 1998.
- Fu, Z.-H., Qiu, K.-B., and Zha, H. Generalize a small pre-trained model to arbitrarily large tsp instances. In *Proceedings of the AAAI conference on artificial intelligence*, volume 35, pp. 7474–7482, 2021.
- Grinsztajn, N., Furelos-Blanco, D., and Barrett, T. D. Population-based reinforcement learning for combinatorial optimization. *arXiv preprint arXiv:2210.03475*, 2022.
- Helsgaun, K. An extension of the lin-kernighan-helsgaun tsp solver for constrained traveling salesman and vehicle routing problems. 12 2017. doi: 10.13140/RG.2.2.25569.40807.
- Hottung, A. and Tierney, K. Neural large neighborhood search for the capacitated vehicle routing problem. *CoRR*, abs/1911.09539, 2019. URL <http://arxiv.org/abs/1911.09539>.
- Hottung, A., Kwon, Y.-D., and Tierney, K. Efficient active search for combinatorial optimization problems. In *International Conference on Learning Representations*, 2021.
- Hou, Q., Yang, J., Su, Y., Wang, X., and Deng, Y. Generalize learned heuristics to solve large-scale vehicle routing problems in real-time. In *The Eleventh International Conference on Learning Representations*, 2022.

- Ioffe, S. and Szegedy, C. Batch normalization: Accelerating deep network training by reducing internal covariate shift. In *International conference on machine learning*, pp. 448–456. pmlr, 2015.
- Jang, H., Kim, M., and Ahn, S. Learning energy decompositions for partial inference of GFlowNets. *International Conference on Learning Representations (ICLR)*, 2024.
- Jin, Y., Ding, Y., Pan, X., He, K., Zhao, L., Qin, T., Song, L., and Bian, J. Pointerformer: Deep reinforced multi-pointer transformer for the traveling salesman problem. *arXiv preprint arXiv:2304.09407*, 2023.
- Joshi, C. K., Cappart, Q., Rousseau, L.-M., and Laurent, T. Learning tsp requires rethinking generalization. In *27th International Conference on Principles and Practice of Constraint Programming (CP 2021)*. Schloss Dagstuhl-Leibniz-Zentrum für Informatik, 2021.
- Khalil, E., Dai, H., Zhang, Y., Dilkina, B., and Song, L. Learning combinatorial optimization algorithms over graphs. *Advances in neural information processing systems*, 30, 2017.
- Kim, H., Kim, M., Ahn, S., and Park, J. Enhancing sample efficiency in black-box combinatorial optimization via symmetric replay training, 2023a.
- Kim, H., Kim, M., Berto, F., Kim, J., and Park, J. Devformer: A symmetric transformer for context-aware device placement. In *International Conference on Machine Learning*, pp. 16541–16566. PMLR, 2023b.
- Kim, M., Park, H., Kim, S., Son, K., Kim, S., Son, K., Choi, S., Park, G., and Kim, J. Reinforcement learning-based auto-router considering signal integrity. In *2020 IEEE 29th Conference on Electrical Performance of Electronic Packaging and Systems (EPEPS)*, pp. 1–3, 2020. doi: 10.1109/EPEPS48591.2020.9231473.
- Kim, M., Park, H., Son, K., Kim, S., Kim, H., Kim, J., Song, J., Ku, Y., Park, J., and Kim, J. Imitation learning for simultaneous escape routing. In *2021 IEEE 30th Conference on Electrical Performance of Electronic Packaging and Systems (EPEPS)*, pp. 1–3, 2021a. doi: 10.1109/EPEPS51341.2021.9609145.
- Kim, M., Park, J., et al. Learning collaborative policies to solve np-hard routing problems. *Advances in Neural Information Processing Systems*, 34:10418–10430, 2021b.
- Kim, M., Park, J., and Park, J. Neuro cross exchange: Learning to cross exchange to solve realistic vehicle routing problems. *arXiv preprint arXiv:2206.02771*, 2022a.
- Kim, M., Park, J., and Park, J. Sym-nco: Leveraging symmetricity for neural combinatorial optimization. *Advances in Neural Information Processing Systems*, 35: 1936–1949, 2022b.
- Kim, M., Ko, J., Zhang, D., Pan, L., Yun, T., Kim, W., Park, J., and Bengio, Y. Learning to scale logits for temperature-conditional GFlowNets. *arXiv preprint arXiv:2310.02823*, 2023c.
- Kim, M., Yun, T., Bengio, E., Zhang, D., Bengio, Y., Ahn, S., and Park, J. Local search gflownets. *arXiv preprint arXiv:2310.02710*, 2023d.
- Kipf, T. N. and Welling, M. Semi-supervised classification with graph convolutional networks. *arXiv preprint arXiv:1609.02907*, 2016.
- Kool, W., van Hoof, H., and Welling, M. Attention, learn to solve routing problems! In *International Conference on Learning Representations*, 2018.
- Kool, W., van Hoof, H., Gromicho, J., and Welling, M. Deep policy dynamic programming for vehicle routing problems. In *International conference on integration of constraint programming, artificial intelligence, and operations research*, pp. 190–213. Springer, 2022.
- Kwon, Y.-D., Choo, J., Kim, B., Yoon, I., Gwon, Y., and Min, S. Pomo: Policy optimization with multiple optima for reinforcement learning. *Advances in Neural Information Processing Systems*, 33:21188–21198, 2020.
- Lin, S. and Kernighan, B. W. An effective heuristic algorithm for the traveling-salesman problem. *Operations research*, 21(2):498–516, 1973.
- Loshchilov, I. and Hutter, F. Sgdr: Stochastic gradient descent with warm restarts. *arXiv preprint arXiv:1608.03983*, 2016.
- Loshchilov, I. and Hutter, F. Decoupled weight decay regularization. *arXiv preprint arXiv:1711.05101*, 2017.
- Luo, F., Lin, X., Liu, F., Zhang, Q., and Wang, Z. Neural combinatorial optimization with heavy decoder: Toward large scale generalization. *arXiv preprint arXiv:2310.07985*, 2023.
- Ma, Y., Li, J., Cao, Z., Song, W., Zhang, L., Chen, Z., and Tang, J. Learning to iteratively solve routing problems with dual-aspect collaborative transformer. *Advances in Neural Information Processing Systems*, 34:11096–11107, 2021.
- Ma, Y., Li, J., Cao, Z., Song, W., Guo, H., Gong, Y., and Chee, Y. M. Efficient neural neighborhood search for pickup and delivery problems. *arXiv preprint arXiv:2204.11399*, 2022.

- Ma, Y., Cao, Z., and Chee, Y. M. Learning to search feasible and infeasible regions of routing problems with flexible neural k-opt. *arXiv preprint arXiv:2310.18264*, 2023.
- Madan, K., Rector-Brooks, J., Korablyov, M., Bengio, E., Jain, M., Nica, A., Bosc, T., Bengio, Y., and Malkin, N. Learning GFlowNets from partial episodes for improved convergence and stability. *International Conference on Machine Learning (ICML)*, 2022.
- Malkin, N., Jain, M., Bengio, E., Sun, C., and Bengio, Y. Trajectory balance: Improved credit assignment in gflownets. *Advances in Neural Information Processing Systems*, 35:5955–5967, 2022.
- Mnih, V., Kavukcuoglu, K., Silver, D., Graves, A., Antonoglou, I., Wierstra, D., and Riedmiller, M. Playing atari with deep reinforcement learning. *arXiv preprint arXiv:1312.5602*, 2013.
- Nazari, M., Oroojlooy, A., Snyder, L., and Takác, M. Reinforcement learning for solving the vehicle routing problem. *Advances in neural information processing systems*, 31, 2018.
- Pan, L., Zhang, D., Courville, A., Huang, L., and Bengio, Y. Generative augmented flow networks. In *The Eleventh International Conference on Learning Representations*, 2022.
- Pan, L., Malkin, N., Zhang, D., and Bengio, Y. Better training of gflownets with local credit and incomplete trajectories. *arXiv preprint arXiv:2302.01687*, 2023a.
- Pan, X., Jin, Y., Ding, Y., Feng, M., Zhao, L., Song, L., and Bian, J. H-tsp: Hierarchically solving the large-scale travelling salesman problem. *arXiv preprint arXiv:2304.09395*, 2023b.
- Park, H., Kim, M., Kim, S., Kim, K., Kim, H., Shin, T., Son, K., Sim, B., Kim, S., Jeong, S., Hwang, C., and Kim, J. Transformer network-based reinforcement learning method for power distribution network (pdn) optimization of high bandwidth memory (hbm). *IEEE Transactions on Microwave Theory and Techniques*, 70(11):4772–4786, 2022. doi: 10.1109/TMTT.2022.3202221.
- Qiu, R., Sun, Z., and Yang, Y. Dimes: A differentiable meta solver for combinatorial optimization problems. *Advances in Neural Information Processing Systems*, 35: 25531–25546, 2022.
- Rector-Brooks, J., Madan, K., Jain, M., Korablyov, M., Liu, C.-H., Chandar, S., Malkin, N., and Bengio, Y. Thompson sampling for improved exploration in GFlowNets. *arXiv preprint arXiv:2306.17693*, 2023.
- Son, J., Kim, M., Choi, S., and Park, J. Solving np-hard min-max routing problems as sequential generation with equity context. *arXiv preprint arXiv:2306.02689*, 2023a.
- Son, J., Kim, M., Kim, H., and Park, J. Meta-sage: scale meta-learning scheduled adaptation with guided exploration for mitigating scale shift on combinatorial optimization. In *International Conference on Machine Learning*, pp. 32194–32210. PMLR, 2023b.
- Stützle, T. and Hoos, H. H. Max–min ant system. *Future Generation Computer Systems*, 16 (8):889–914, 2000. ISSN 0167-739X. doi: [https://doi.org/10.1016/S0167-739X\(00\)00043-1](https://doi.org/10.1016/S0167-739X(00)00043-1). URL <https://www.sciencedirect.com/science/article/pii/S0167739X00000431>.
- Sun, H., Goshvadi, K., Nova, A., Schuurmans, D., and Dai, H. Revisiting sampling for combinatorial optimization. In Krause, A., Brunskill, E., Cho, K., Engelhardt, B., Sabato, S., and Scarlett, J. (eds.), *Proceedings of the 40th International Conference on Machine Learning Research*, volume 202 of *Proceedings of Machine Learning Research*, pp. 32859–32874. PMLR, 23–29 Jul 2023. URL <https://proceedings.mlr.press/v202/sun23c.html>.
- Sun, Z. and Yang, Y. Difusco: Graph-based diffusion solvers for combinatorial optimization. *arXiv preprint arXiv:2302.08224*, 2023.
- Veličković, P., Cucurull, G., Casanova, A., Romero, A., Liò, P., and Bengio, Y. Graph attention networks. In *International Conference on Learning Representations*, 2018.
- Vinyals, O., Fortunato, M., and Jaitly, N. Pointer networks. *Advances in neural information processing systems*, 28, 2015.
- Williams, R. J. Simple statistical gradient-following algorithms for connectionist reinforcement learning. *Machine learning*, 8:229–256, 1992.
- Xin, L., Song, W., Cao, Z., and Zhang, J. Multi-decoder attention model with embedding glimpse for solving vehicle routing problems. In *Proceedings of the AAAI Conference on Artificial Intelligence*, volume 35, pp. 12042–12049, 2021.
- Ye, H., Wang, J., Cao, Z., Liang, H., and Li, Y. Deepaco: Neural-enhanced ant systems for combinatorial optimization. *arXiv preprint arXiv:2309.14032*, 2023.
- Ye, H., Wang, J., Liang, H., Cao, Z., Li, Y., and Li, F. Glop: Learning global partition and local construction for solving large-scale routing problems in real-time. In *Proceedings of the AAAI Conference on Artificial Intelligence*, 2024.

- Zhang, C., Song, W., Cao, Z., Zhang, J., Tan, P. S., and Chi, X. Learning to dispatch for job shop scheduling via deep reinforcement learning. *Advances in Neural Information Processing Systems*, 33:1621–1632, 2020.
- Zhang, D., Malkin, N., Liu, Z., Volokhova, A., Courville, A., and Bengio, Y. Generative flow networks for discrete probabilistic modeling. In *International Conference on Machine Learning*, pp. 26412–26428. PMLR, 2022a.
- Zhang, D., Dai, H., Malkin, N., Courville, A., Bengio, Y., and Pan, L. Let the flows tell: Solving graph combinatorial optimization problems with gflownets. *arXiv preprint arXiv:2305.17010*, 2023a.
- Zhang, D., Pan, L., Chen, R. T. Q., Courville, A. C., and Bengio, Y. Distributional gflownets with quantile flows. *Transactions on Machine Learning Research*, abs/2302.05793, 2023b.
- Zhang, D. W., Rainone, C., Peschl, M., and Bondesan, R. Robust scheduling with gflownets. In *The Eleventh International Conference on Learning Representations*, 2022b.

## A. Implementation

### A.1. Learning architecture and optimizer

We utilize the anisotropic graph neural network with edge gating mechanisms, which is proposed by (Joshi et al., 2021) and adopted by (Ye et al., 2023), as the foundational GNN architecture for the construction of a heuristic matrix. This network offers node and edge embeddings that are more beneficial for edge prediction than other popular GNN variants, such as Graph Attention Networks (Veličković et al., 2018) or Graph Convolutional Networks (Kipf & Welling, 2016).

We represent the node feature of node  $v_i$  at the  $\ell$ -th layer as  $h_i^\ell$ , and the feature of the edge between nodes  $i$  and  $j$  at the same layer as  $e_{ij}^\ell$ . These features undergo propagation to the next layer  $\ell + 1$  through an anisotropic message passing scheme, detailed as follows:

$$h_i^{\ell+1} = h_i^\ell + \alpha(\text{BN}(U^\ell h_i^\ell + \mathcal{A}_{j \in \mathcal{N}_i}(\sigma(e_{ij}^\ell) \odot V^\ell h_j^\ell))) \quad (13)$$

$$m^\ell = P^\ell e_{ij}^\ell + Q^\ell h_i^\ell + R^\ell h_j^\ell \quad (14)$$

$$e_{ij}^{\ell+1} = e_{ij}^\ell + \alpha(\text{BN}(m^\ell)) \quad (15)$$

where  $U^\ell, V^\ell, P^\ell, Q^\ell, R^\ell \in R^{d \times d}$  are the learnable parameters of layer  $\ell$ ,  $\alpha$  denotes the activation function,  $\text{BN}$ (Ioffe & Szegedy, 2015) denotes batch normalization,  $\mathcal{A}$  denote the aggregation function,  $\sigma$  is the sigmoid function,  $\odot$  is Hadamard product,  $\mathcal{N}_i$  denotes the neighborhoods of node  $v_i$ . In this paper we use  $\alpha$  is SiLU(Elfwing et al., 2018) and  $\mathcal{A}$  is mean pooling. We transform the extracted edge features into real-valued heuristic metrics by employing a 3-layer Multilayer Perceptron (MLP) that includes skipping connections to the embedded node feature  $h$ . The SiLU is the activation function for all layers except the output layer, in which the sigmoid function is applied to generate normalized outputs. The training process is optimized using the AdamW optimizer(Loshchilov & Hutter, 2017) in conjunction with a Cosine Annealing Scheduler(Loshchilov & Hutter, 2016)

### A.2. Hyperparameters

For a task of COP (e.g., TSP200), we train GFACS for  $N_{\text{epoch}}$  epochs. In each epoch, we use  $N_{\text{inst}}$  number of instances using mini-batch with size  $M$ ; thus  $N_{\text{inst}}/M$  gradient steps are taken per epoch. For each problem instance, we sample  $K$  solutions to train with, as discussed in Section 5.1. Our main baseline algorithm, DeepACO, is also trained using the same hyperparameters to ensure a fair comparison. We summarize used value for  $N_{\text{epoch}}$ ,  $N_{\text{inst}}$ ,  $M$  and  $K$  in Table 4. Note that for TSP1000 and CVRP1000, we use model checkpoints pre-trained in TSP500 and CVRP500, respectively, to reduce the processing time for training.

Table 4. Training hyperparameter settings for each task. These hyperparameter settings are used both for GFACS and DeepACO training. The values with \* indicate that the values are used for fine-tuning a pre-trained model.

	TSP200	TSP500	TSP1000	CVRP200	CVRP500	CVRP1000	OP100	PCTSP100	SOP100	SMTWTP100	BPP120
$N_{\text{epoch}}$	50	50	20*	50	50	20*	20	20	20	20	20
$N_{\text{inst}}$	400	400	200*	200	200	100*	100	100	100	100	100
$M$	20	20	10	10	10	5	5	5	5	5	5
$K$	30	30	20	20	20	15	30	30	30	30	30

There are other hyperparameters to be considered specifically for GFACS.  $\beta$  is one of the most important hyperparameters for training GFACS, which is analyzed in Section 6.3. As we’ve discussed in Section 5.1, we use annealing for  $\beta$  using the following log-shaped scheduling:

$$\beta = \beta_{\min} + (\beta_{\max} - \beta_{\min}) \min \left( \frac{\log(i_{\text{epoch}})}{\log(N_{\text{epoch}} - N_{\text{flat}})}, 1 \right)$$

where  $i_{\text{epoch}}$  is the index of epoch and  $N_{\text{flat}}$  is the number of last epochs to have  $\beta = \beta_{\max}$ .

We report the  $\beta$  value used for each task in Table 5. Note that  $\beta$  remains consistent across different scales of the same problem class.

*Table 5. Settings of  $\beta$  for each task.*

	TSP	CVRP	OP	PCTSP	SOP	SMTWTP	BPP
$\beta_{\min}$	200	500	5	20	10	10	500
$\beta_{\max}$	1000	2000	10	50	20	20	5000

For TSP and CVRP, where we have local search operators, we also need  $\alpha$  for energy reshaping (Eq. 9). We empirically found that linearly increasing  $\alpha$  from 0.5 to 1.0 along the epochs works well, and we use that setting for all TSP and CVRP experiments.

### A.3. Computing resource

Throughout the experiments, we utilize a single CPU, specifically an AMD EPYC 7542 32-Core Processor, and a single GPU, the NVIDIA RTX A6000, for training neural networks. After that, the inference was conducted on a separate, standalone PC with a single AMD Ryzen 9 5900X 12-Core Processor and NVIDIA RTX 4070 Ti to assess the wall time of each algorithm fairly.

### A.4. Hyperparameters for LKH-3.

LKH-3 (Helsgaun, 2017), an extension of the Lin-Kernighan heuristic (Lin & Kernighan, 1973), is a powerful open-source heuristic solver designed for solving routing problems. It not only addresses TSP but also handles a wide array of constrained routing problems, such as CVRP and PDP, by minimizing a penalty term that measures constraint violations.

In the following, we describe the parameter settings for LKH-3 used in this work. For both TSP and CVRP, we set `MAX_TRIALS` to be  $100 \times N$  where  $N$  is the number of nodes and `SEED` to 1234. We set `RUNS` to 10 for TSP but 1 for CVRP to limit the search time in a reasonable range. For other parameters not stated, we followed the default settings.

## B. Problem Settings

In this section, we provide an overview of the combinatorial optimization problems we address. These encompass vehicle routing problems, bin packing problems, and scheduling problems. For a comprehensive understanding of each problem’s specific settings, we direct readers to the work by [Ye et al. \(2023\)](#). Furthermore, for access to the exact source code pertaining to each problem, please refer to the repository available at <sup>2</sup> from [Ye et al. \(2023\)](#).

**Traveling Salesman Problem** In the Traveling Salesman Problem (TSP), we aim to find the shortest route that visits a set of nodes once and returns to the origin. We consider Euclidean TSP, where the distance between two nodes is determined by Euclidean distance. A TSP instance can be determined as a set of nodes with 2D coordinates. We generate a random TSP instance by sampling the coordinate from a unit square,  $[0, 1]^2$ .

**Capacitated Vehicle Routing Problem** Similar to TSP, Capacitated Vehicle Routing Problem (CVRP) also seeks the shortest path that visits all the nodes once. In CVRP, however, a vehicle has a limited capacity, and each node has a demand to be satisfied. The sum of the demand of each subroute should not exceed the capacity, which limits the number of nodes that can be visited by one vehicle. In our setting, CVRP is also defined in Euclidean space.

A CVRP instance can be represented by a set of customer nodes, a single depot node, and a capacity  $C$ . Each customer node has a position (2D coordinates) and a demand, while the depot only has a position. A random CVRP instance is generated by sampling the coordinates of both customer and depot from a unit square  $[0, 1]^2$  and sampling demands for each customer from a predefined uniform distribution,  $U[a, b]$ . We use  $a = 1$  and  $b = 9$ , and a fixed  $C = 50$  for all problem scales, 200, 500 and 1000.

**Orienteering Problem** In the Orienteering Problem (OP), the objective is to maximize the total prize of visited nodes within a given tour length limitation. This problem is similar to CVRP but focuses on maximizing gains rather than minimizing costs.

An OP instance comprises a set of nodes to visit, each with its position and prize, a depot, and a maximum length constraint. We sample a random OP instance by first sampling the position of nodes, including the starting node, from a unit square  $[0, 1]^2$ . And we set the prize for each node, following ([Fischetti et al., 1998](#); [Ye et al., 2023](#)), to be  $p_i = (1 + \lfloor 99 \cdot \frac{d_{0,i}}{\max_{j=1}^n d_{0,j}} \rfloor) / 100$ , where  $d_{0,i}$  is the Euclidean distance from the depot to node  $i$ . We set the maximum length to 4 in the OP100 task, following [Kool et al. \(2018\)](#).

**Prize-Collecting Traveling Salesman Problem** The Prize-Collecting Traveling Salesman Problem (PCTSP) extends the TSP by associating a prize for visiting a node and a penalty for not visiting it. The goal is to find a tour that minimizes the total travel cost plus penalties for the unvisited nodes and also satisfies a predefined prize threshold. In PCTSP, balancing the need to collect prizes against the cost of visiting more nodes matters.

A PCTSP instance comprises a set of nodes to visit, a depot, and a minimum total prize threshold. The coordinates of nodes and depot are sampled in the unit square. The prize for each node is sampled from  $U[0, 1]$ , while the penalty for each node is sampled from  $U[0, C_N]$ , where  $C_N$  is set to 0.12 for  $N = 100$ . Lastly, the minimum total prize threshold is  $N/4$  for problems with  $N$  nodes, i.e., 25 for PCTSP100.

**Sequential Ordering Problem** The Sequential Ordering Problem (SOP) seeks to find a linear order of jobs that minimizes total processing time with a set of precedence constraints among the jobs. An SOP instance is a set of jobs and precedence constraints. Each job has its own processing time, and each pair has a waiting (transition) time.

We sample an SOP instance by sampling the processing time and waiting time from  $U[0, 1]$ . The precedence constraints for each job pair are laid with probability 0.2, while ensuring feasibility, i.e., when  $i < j$  means that the constraint that job  $i$  precedes the job  $j$ , the feasibility of a problem requires  $i < j$  and  $j < k$  then  $i < k$ .

**Single Machine Total Weighted Tardiness Problem** This problem involves scheduling jobs on a single machine where each job has a due date, processing time, and weight. The objective is to minimize the total weighted tardiness, which is the sum of the weights of the jobs multiplied by their tardiness (the amount of time a job is completed after its due date).

<sup>2</sup><https://github.com/henry-yeh/DeepACO>

To generate an SMTWTP instance, we sample a due date from  $U[0, N]$ , the weight from  $U[0, 1]$ , and the processing time from  $U[0, 2]$ , where  $N$  is the number of jobs to process.

**Bin Packing Problem** The Bin Packing Problem (BPP) involves packing objects of different volumes into a finite number of bins or containers of fixed capacity to minimize the number of bins used. In this work, we use the latter setting.

To generate a BPP instance, we sample the  $N$  items with a random size from  $U[20, 100]$ . And we use 150 for the bin capacity.



## C. Additional Experiments

### C.1. Experiments on TSPLIB

This section presents a comparison of performance between the baseline models and our model on real-world Traveling Salesman Problem (TSP) instances. We evaluated the models on TSP200, TSP500, and TSP1000 under their respective conditions. Our model outperforms the other Ant Colony Optimization (ACO) baselines, demonstrating superior generalization capabilities.

Table 6. Evaluation of ACO methods on the real-world TSP problem. ‘#’ denotes the number of instances in each set.

Size	#	ACO	DeepACO	Ours
$100 \leq N < 300$	30	1.71%	1.25%	<b>1.21%</b>
$300 \leq N < 700$	10	4.26%	2.70%	<b>2.60%</b>
$700 \leq N < 1500$	12	7.01%	4.08%	<b>3.88%</b>
ALL	52	3.43%	2.24%	<b>2.16%</b>

### C.2. Comparison against TAM

We compare GFACS and DeepACO against CVRP instances used in TAM (Hou et al., 2022). These instances have a different capacity constraint from those we used for the main experiment. Please refer to (Hou et al., 2022) for more details regarding the instance generation. Moreover, to match the processing time to be comparative to DeepACO, we set  $K$  (equal to the number of ants for ACO) to 16.

Table 7. Results for CVRP instances used in TAM. The result for AM and TAM is drawn from Hou et al. (2022), and the result for DeepACO is drawn from Ye et al. (2023).

Method	CVRP100		CVRP400	
	Obj.	Time (s)	Obj.	Time (s)
AM*	16.42	0.06	29.33	0.20
TAM*	16.08	0.086	25.93	1.35
DeepACO ( $T = 4$ )	16.08	2.97	25.31	3.65
DeepACO ( $T = 10$ )	15.77	3.87	25.27	5.89
GFACS ( $T = 4$ )	15.77	1.07	24.95	3.23
GFACS ( $T = 10$ )	15.72	1.40	24.87	5.21

## D. Diversity Calculation

The diversity of  $K$  solutions generated from a solver is defined as the average pairwise Jaccard distance,  $\frac{1}{K(K-1)} \sum_i \sum_j d_J(x_i, x_j)$ , where  $d_J$  is defined as follows:

$$d_J(x_i, x_j) = 1 - J(x_i, x_j) = 1 - \frac{|E(x_i) \cap E(x_j)|}{|E(x_i) \cup E(x_j)|} \quad (16)$$

where  $E_x$  is the set of edges composing the solution  $x$ . In TSP or CVRP, the (undirected) edge is a set of adjoining nodes in the solution path.

## E. Symmetric Solutions of Combinatorial Optimization

This section delves into the symmetric characteristics of combinatorial solutions, wherein multiple trajectories, denoted as  $\tau$ , can map to an identical combinatorial solution. We begin with a formal analysis focusing on two quintessential tasks: the Traveling Salesman Problem (TSP) and the Capacitated Vehicle Routing Problem (CVRP). This analysis lays the foundation for understanding the connections to other related combinatorial optimization problems.

**Proposition E.1** (Symmetry Solution in TSP (Hamiltonian Cycle)). *Let  $\mathcal{G} = (\mathcal{V}, \mathcal{D})$  be a finite, undirected graph where  $\mathcal{V}$  is the set of vertices and  $\mathcal{D}$  is the set of edges. Assume  $\mathcal{G}$  contains a Hamiltonian cycle. Denote  $N = |\mathcal{V}|$  as the number of vertices. If  $N > 1$ , there exist exactly  $2N$  symmetric trajectories (including the cycle and its reverse) starting from each vertex in the cycle. For  $N = 1$ , there is exactly one identical trajectory.*

*Proof.* A Hamiltonian cycle in  $\mathcal{G}$  is a cycle that visits every vertex exactly once. For  $N > 1$ , each cycle can be traversed in two distinct directions (clockwise and counterclockwise) from each vertex, yielding 2 trajectories per vertex. Since there are  $N$  vertices, this results in  $2N$  symmetric trajectories. For  $N = 1$ , the cycle is trivial and only has one trajectory.  $\square$

**Proposition E.2** (Symmetric Solutions in CVRP). *Consider a Capacitated Vehicle Routing Problem (CVRP) defined on a graph  $\mathcal{G} = (\mathcal{V}, \mathcal{D})$  with a designated depot vertex. Let there be  $K$  distinct Hamiltonian cycles (or routes) originating and terminating at the depot, and denote  $S$  as the number of single vertex cycles (excluding the depot) among these  $K$  cycles. The total number of symmetric solutions, considering the directionality of each cycle, is given by  $K! \times 2^{K-S}$ .*

*Proof.* Each of the  $K$  cycles can be ordered in  $K!$  ways. Excluding the  $S$  single vertex cycles, each of the remaining  $K - S$  cycles can be traversed in two directions (forward and reverse). Therefore, for these  $K - S$  cycles, there are  $2^{K-S}$  ways to choose a direction. The product  $K! \times 2^{K-S}$  gives the total number of symmetric solutions for the CVRP under these conditions.  $\square$

The propositions discussed previously can be extended to various variants of vehicle routing problems. Specifically, in the context of the orienteering problem (OP) and prize collecting Traveling Salesman Problem (PCTSP), which represent special cases where  $K = 1$ , the number of symmetric trajectories is determined by the number of vertices,  $N$ , in the solution. When  $N > 1$ , there are exactly 2 symmetric trajectories for each route. In contrast, for a single-vertex solution ( $N = 1$ ), the trajectory is identical, reflecting the singularity of the route.

## F. Extended Related Works

### F.1. Deep Constructive Policy for Neural Combinatorial Optimization

Constructive policy methods systematically build solutions by incrementally adding elements, beginning with an empty set and culminating in a complete solution. This approach ensures compliance with constraints by progressively narrowing the scope of actions, making it versatile for application in domains like vehicle routing (Nazari et al., 2018), graph combinatorial optimization (Khalil et al., 2017), and scheduling (Zhang et al., 2020).

In deep learning, various techniques adopt this constructive policy framework. Notably, the attention model (AM) (Kool et al., 2018) has been pivotal in vehicle routing problems (VRPs), establishing a new standard for stabilizing REINFORCE training. Subsequent advancements in AM have included enhanced decoder architecture (Son et al., 2023a; Xin et al., 2021; Luo et al., 2023), improved REINFORCE (Williams, 1992) baseline assessments (Kwon et al., 2020; Kim et al., 2022b), leveraging symmetries for sample efficiency (Kim et al., 2023a), the application of population-based reinforcement learning (RL) (Grinsztajn et al., 2022), and refined solution-building methods (Drakulic et al., 2023). Recent advancements in hierarchical algorithms exploit AM-based policies for solution optimization: one policy broadly generates solutions while another refines them locally (Kim et al., 2021b; Hou et al., 2022; Ye et al., 2024). Additionally, AM-driven constructive policies have been effectively applied in hardware routing (Kim et al., 2020; 2021a) and placement tasks (Park et al., 2022; Kim et al., 2023b).

Graph combinatorial optimization, particularly in problems like maximum independent sets, has diversified from contrive VRPs policies due to their local decomposability and the relative ease of training value functions for partial solutions where VRPs are not locally decomposable due to their global contains. Starting with the influential works by Khalil et al. (2017), which employed deep Q networks (Mnih et al., 2013) for graph policy training, creating solutions constructively, Ahn et al. (2020) introduced an innovative Markov Decision Process (MDP) to generate multiple solution components per iteration by exploiting the local decomposability of graph combinatorial problems. Zhang et al. (2023a) further developed this concept, training their MDP with forward-looking GFlowNets (Pan et al., 2023a).

Our research aligns with the deep constructive policy framework, where GFlowNets constructively build actions from an initial empty solution ( $s_0$ ) to a final complete solution ( $s_n$ ). Additionally, our methods include a heatmap-based approach, detailed in Appendix F.3.

### F.2. Deep Improvement Policy for Neural Combinatorial Optimization

The improvement policy focuses on refining complete solutions, similar to local search methods like 2opt (Croes, 1958). Its advantage lies in achieving comparable performances to constructive policies, especially when allotted sufficient time for extensive improvement iterations. Researchers typically adapt existing heuristic local search techniques, creating learning policies that emulate these methods through maximizing expected returns via reinforcement learning (d O Costa et al., 2020; Hottung & Tierney, 2019; Ma et al., 2021; 2022; 2023; Kim et al., 2022a). Also, recent works have explored active search to refine solutions via policy adjustments (Hottung et al., 2021; Son et al., 2023b). Moreover, alternative strategies using discrete Langevin sampling instead of neural networks have shown promising outcomes (Sun et al., 2023). This approach serves as a complementary extension to deep constructive policies, as it often enhances solutions initially formulated by constructive methods. Additionally, our method, which integrates local search into the training loop, could see further enhancements if advancements in this area are incorporated into our training procedures.

### F.3. Heatmap-based Neural Combinatorial Optimization

The heatmap-based method (Joshi et al., 2021) entails the acquisition of a graph representation, referred to as the ‘‘Heatmap,’’ from input graph instances. This Heatmap serves as a prior distribution, influencing the generation of a solution. However, this approach is not self-contained and requires an additional solution construction step, which may involve techniques like beam search (Joshi et al., 2021), dynamic programming (Kool et al., 2022), or Monte Carlo tree search (Fu et al., 2021; Qiu et al., 2022; Sun & Yang, 2023). The key advantage of the heatmap-based method lies in its exceptional generalizability when compared to constructive policies. It operates at an abstract level, free from the constraints inherent in generating actual combinatorial solutions.

Our approach falls under heatmap-based methodologies, where we learn a heuristic metric (i.e., heatmap) and employ ant colony optimization for solution construction. A key advantage of our method over many other supervised learning-based heatmap approaches is its independence from optimally labeled data.